Spectroscopy and thermal properties of Ga2S3 based glasses

Article *in* Journal of Non-Crystalline Solids · June 1999

DOI: 10.1016/S0022-3093(99)00061-7

ELSEVIER

Journal of Non-Crystalline Solids 247 (1999) 189–195

JOURNAL OF NON-CRYSTALLINE SOLIDS

Spectroscopy and thermal properties of Ga_2S_3 based glasses

E.M. Marmolejo [a], E. Granado [a], O.L. Alves [b], C.L. Cesar [a], L.C. Barbosa [a,*]

[a] *State University of Campinas, Institute of Physics Gleb Wataghin, Department of Quantum Electronics, P.O. Box 6165, 13083-970, Campinas, SP, Brazil*

[b] *Institute of Chemistry, P.O. Box 6164, 13083-970, Campinas, SP, Brazil*

Abstract

In the present work we describe the synthesis and spectroscopy and thermal properties of the vitreous system $20La_2S_3$–$(80 - x)Ga_2S_3$–xCsCl, x varying from 10 to 30, producing homogeneous glasses by fusion method in vitreous carbon crucible in a horizontal silica chamber with a controlled atmosphere of sulphur, present during whole process. The sample properties, after synthesis, were measured by X-ray diffratometry, absorption spectroscopy, Raman scattering, density, hardness and refractive index. Our results show that the density, refractive index and hardness increase with CsCl content, while the phonon frequencies are less than 470 cm^{-1}. We have drawn optical fibers from samples in this glass system because of an increase of thermal stability with increasing CsCl content. The refractive index measurements allowed us to estimate the third-order non-linear optical susceptibilities and show that it depends on the CsCl content.

1. Introduction

Chalcogenide glasses of the family Ga_2S_3–La_2S_3 (GLS) attracted interest due to the possibility of their use as a host for praseodymium or dysprosium in an optical amplifier for the 1.3 μm wavelength communication window. From its phonon frequency of 430 cm^{-1} and refractive indices, varying from 2.1 to 2.5, we expect long excited state lifetimes which increase the pump efficiency [1–3]. However, because the temperature for a viscosity suitable for fiber drawing was below the onset of crystallization, it was not possible to obtain optical fibers out of them [4]. The addition of CsCl in the glass composition increases the thermal stability region making it possible to draw optical fibers from the glasses of this system [5]. In this paper we measure the glass density, refractive index, hardness and phonon frequencies as a function of the CsCl content in the glass. Our results show that the density, refractive index and hardness increase with CsCl content, while the phonon frequencies are less than 470 cm^{-1}. From the refractive index data we use the Lines model [6,7] to estimate the third order non-linear optical susceptibility $\chi^{(3)}$ we suggest that the CsCl addition can increase $\chi^{(3)}$ from $\sim 4.5 \times 10^{-12}$ to $\sim 5.6 \times 10^{-12}$ esu, desirable for optical devices [7].

2. Experimental procedure

The $20La_2S_3$–$(80 - x)Ga_2S_3$–xCsCl glass system samples with x varying from 10 to 30, were fabricated using a new technique, which reduces hydrogen impurities, obtaining glasses with high optical quality. The conventional way of melting chalcogenide glasses is by batching the glass in a

* Corresponding author. Tel.: +55-19 788 5429; fax: +55-19 289 2883; e-mail: barbosa@ifi.unicamp.br

0022-3093/99/$ – see front matter
PII: S0022-3093(99)00061-7

vitreous carbon crucible placed inside a fused silica tube, which is sealed after evacuating to a pressure of about 10^{-5} Torr and heated to a temperature between 1100 and 1200°C. In this new technique, the problem of explosion of the sealed silica ampoule is solved, by using a horizontal furnace with a silica tube liner, in which we can control the atmosphere under flowing argon condition. To avoid loss of sulphur during the melting process we placed a crucible containing, typically, 20 g of pure sulphur in another furnace, away from the melting zone. The concentration of sulphur vapor across the melting zone was established by the temperature of the second furnace and the carrier argon gas flux. A bubble maker containing ~7 cm of sodium hydroxide solution provided a back pressure within the tube and eliminated H_2S pollution. Melting was achieved at 1150°C during 6 h. After this time the vitreous carbon with the liquid glass was removed from the melting zone by a device and placed where it could be removed by suction to another furnace where it was annealed during 48 h at 400°C. Fig. 1 shows the experimental set up of the melting process. Table 1 shows the composition of the glass batch (CERAC, 99.99% pure).

The refractive indices were measured over a wavelength range from 680–1750 nm using a manual Rudolph null ellipsometer (model 436) with a 150 W tungsten lamp as a light source, with an accuracy of ±0.001. Interference filters selected the desired wavelength. The glassy state was confirmed by X-ray diffraction analysis using CuKα radiation in a diffractometer (Shimadzu). Raman spectra were measured using the 514.5 nm Argon ion laser line at backscattering geometry and triple spectrometer (Jobin–Yvon) with multichannel detection. The density was measured by the Archimeds method. The thermal properties were measured by differential thermal analysis (DTA) (Shimadzu), which provided the characteristic temperatures, and by thermal mechanical analysis (TMA) (Shimadzu), which yielded the coefficient of thermal expansion and softening temperature, both at 10°C/min heating rate. The

Table 1
Glass composition (mol%)

Glass	La_2S_3	Ga_2S_3	CsCl
GLSC10	20	70	10
GLSC20	20	60	20
GLSC30	20	50	30
GLSC40	20	40	40

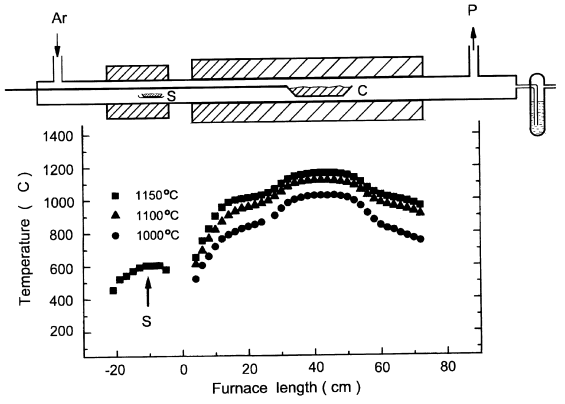

Fig. 1. Set up experimental and temperature profile of the glass samples fabrication. C is a vitreous carbon crucible, S is a silica crucible with sulphur and P is the preform suction vacuum method fabrication.

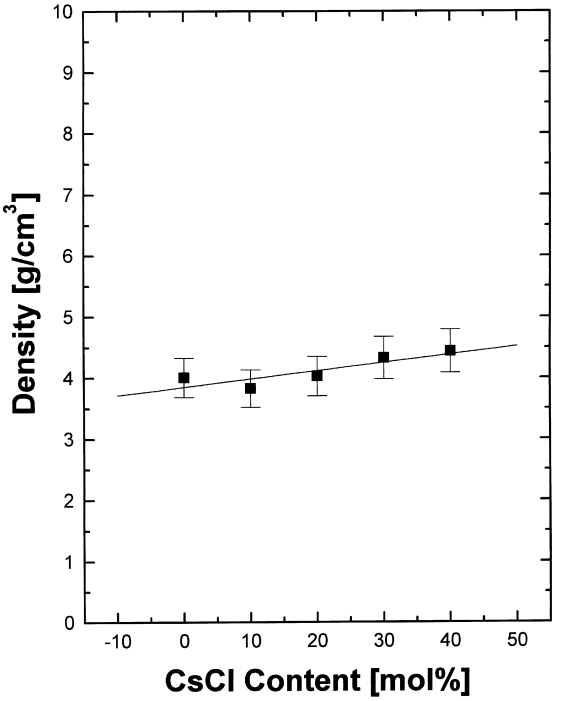

Fig. 2. The Ga_2S_3–La_2S_3–CsCl glass system density dependence on the CsCl content.

micro-hardness was measured with a Vickers equipment, loading was 5 g for 25 s, with ten measurements averaged for each sample. UV-visible spectra were recorded in the wavelength region from 300 to 2500 nm, using a spectrophotometer (Perkin–Elmer Lambda 9).

3. Results

3.1. Glass formation

The preparation procedure, described in the experimental section, allowed us to obtain visually bubble-free transparent glasses with no visual inhomogeneities and a yellowish color. All compositions had the XRD patterns typical for a glass phase presenting a halo near $2\theta = 25°$.

3.2. Thermal properties

Figs. 2 and 3 show the thermal stability and the thermal expansion coefficient as a function of the CsCl content, respectively.

3.3. Refractive index and density

The measured linear refractive index, n, of the glasses decrease with increasing wavelength in the range 300–1750 nm as shown in Fig. 4. We used these measurements to obtain E_ds and E_os by fitting the expression for n as a function of the photon energy E proposed by Wemple [8]

$$1/(n^2 - 1) = E_o/E_d - E^2/(E_o E_d),$$

where E_o is the average excitation energy gap for the optical transitions and E_d represents the electronic dispersion related oscillator strength. The E_os (listed in Table 2) were used to estimate the non-linear refractive index in Section 4.1.

Fig. 5 shows the density as a function of the CsCl content.

3.4. Hardness

Fig. 6 shows the hardness as a function of the CsCl content, where an approximate linear relation between the content of CsCl and the hardness is evident.

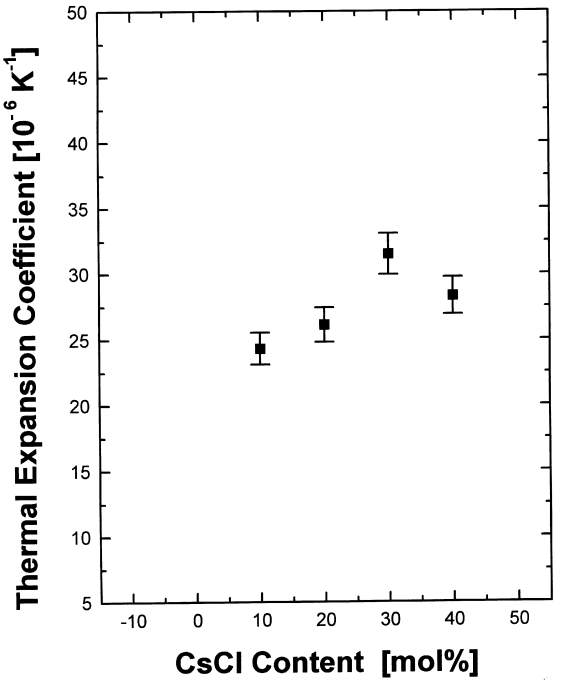

Fig. 3. The thermal expansion coefficient for the Ga_2S_3–La_2S_3–CsCl glass system as a function of the CsCl content (mol%).

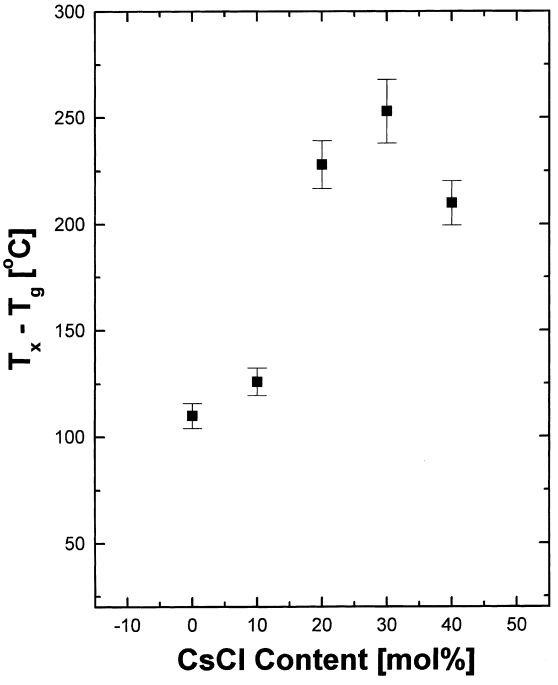

Fig. 4. Thermal stability ($T_x - T_g$) for the Ga_2S_3–La_2S_3–CsCl glass system in function of the CsCl content.

Table 2
Data used to calculate $\chi^{(3)}$ from Lines theory

Glass	CsCl (mol%)	n (1.5 μm)	d (Å) ± 0.1	E_o (eV)	E_d (eV)	$\chi^{(3)}$ (10^{-12} esu)
GLSC10	10	2.253 ± 0.001	2.3 ± 0.1	4.4 ± 0.1	17.3 ± 0.7	4.5 ± 0.2
GLSC20	20	2.265 ± 0.001	2.3 ± 0.1	4.2 ± 0.1	16.7 ± 0.5	5.1 ± 0.3
GLSC30	30	2.322 ± 0.001	2.3 ± 0.1	4.3 ± 0.1	18.2 ± 0.9	5.6 ± 0.6
GLSC40	40	2.379 ± 0.001	2.3 ± 0.1	4.8 ± 0.1	21.9 ± 0.4	5.2 ± 0.2

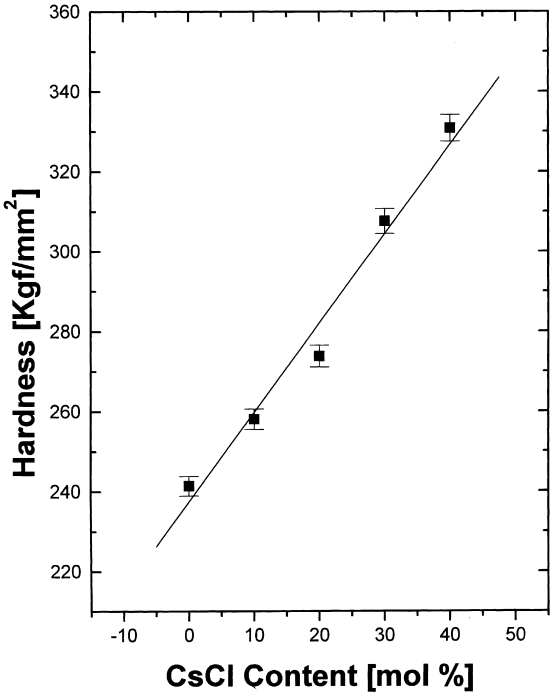

Fig. 5. Hardness for the Ga_2S_3–La_2S_3–CsCl glass system in function of the CsCl concentration in mol%.

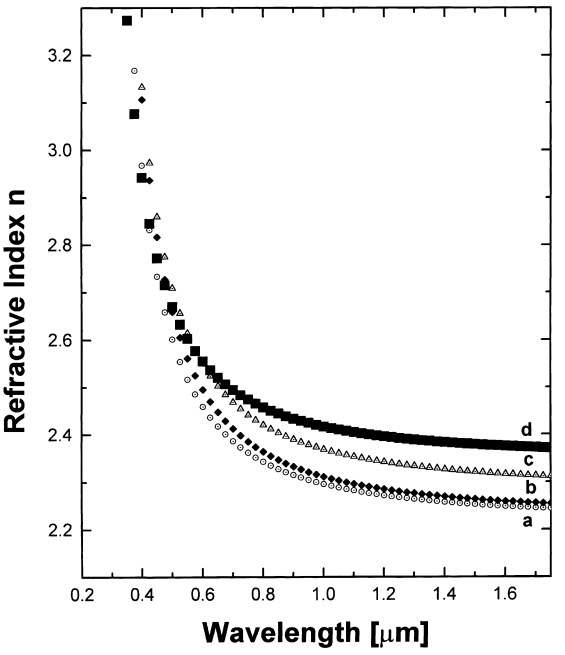

Fig. 6. Linear refractive index as a function of wavelength: a, b, c and d are for 10, 20, 30 and 40 mol% CsCl, respectively.

3.5. Raman spectra

The Raman spectra from the GLSC glasses are presented in Fig. 7, where the boson band, at about 85 cm^{-1} characteristic of the vitreous state, a band at 315 cm^{-1} and the two bands at 230 cm^{-1} and 466 cm^{-1} can be seen. Apparently, there is no effect of the CsCl content on the Raman cut off at 440 cm^{-1}.

3.6. Absorption spectra

The absorption coefficient, α, was measured using two samples with different thickness [9]. The optical gap was assigned to the root of the absorption tail extrapolation in a plot of $\sqrt{(\alpha E)}$ vs E, where E is the photon energy in eV, as done by Tauc [10]. Fig. 8 shows these extrapolations with the corresponding optical gaps defined by $\sqrt{(\alpha E_{opt})} = 0$. There is a red shift as the CsCl content increases.

4. Discussion

4.1. Estimate of non-linear refractive index

Lines [6,7] has analysed the effect of several glass property parameters on the non-linear re-

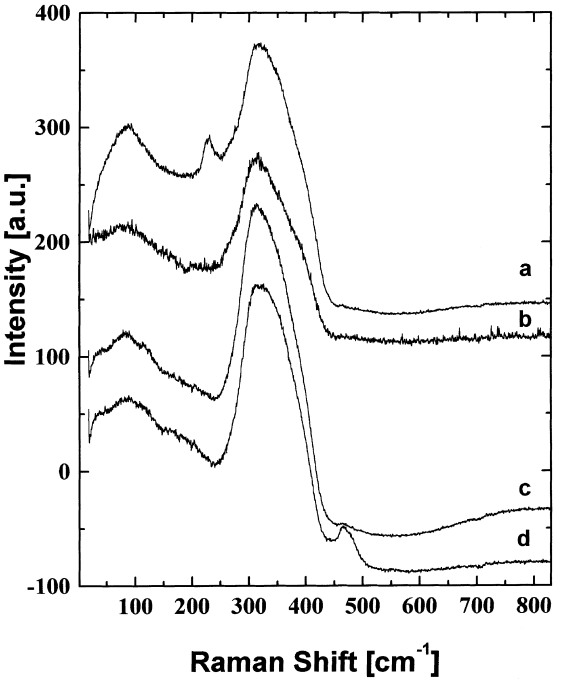

Fig. 7. Raman spectra of GLSC glass system. The spectra have been arbitrarily shifted vertically for clarity: a, b, c and d are for 10, 20, 30 and 40 mol% CsCl, respectively.

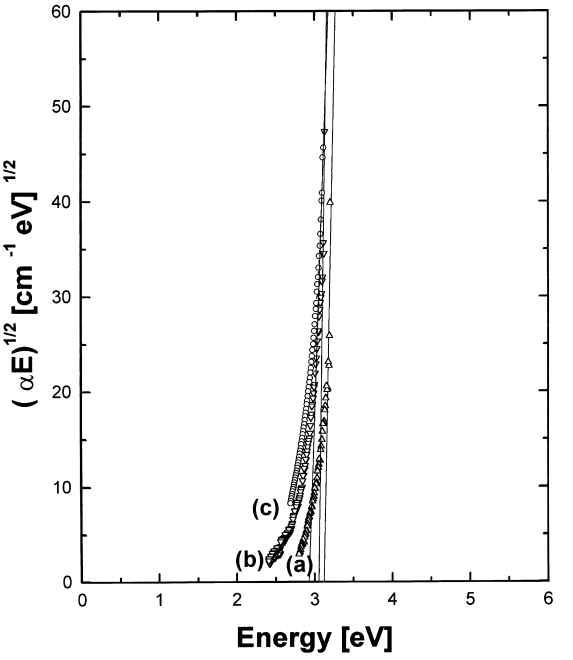

Fig. 8. $\sqrt{\alpha}E$ versus E plot for GLSC glass system. (a) 20 mol% CsCl, (b) 30 mol% CsCl and (d) 40 mol% CsCl, respectively.

fractive index of transparent glass and obtained the following formula for the frequency-dependent non-linear refractive index n_2.

$$n_2(\text{av.})/10^{-13}\ \text{esu} = 25\frac{(f\times f_L)^3 d^2(n^2-1)E_s^6}{n(E_s^2-\hbar^2\omega^2)^4} \quad (1)$$

where d is the bond length for the ternary glass (in Å), f is a local field enhancement factor, $f_L=(n^2+2)/3$ is the Lorentz local-field factor [7], n is the long-wavelength limit of the refractive index, E_s is the effective Sellmeier energy gap. The n_2's at $\lambda=1.5$ μm were estimated with the measured refractive indices, by assuming $f=1$ and making $E_s=E_o$ [6,7]. The bond length, d, for these glasses were estimated to be 0.23 nm using the method proposed by Nassau [11,12]. Finally, $\chi^{(3)}$ is obtained from the n_2 through the equation [7]

$$\chi^{(3)}(-\omega,\omega,\omega,\omega)=\frac{n}{3\pi}n_2(\text{av.}), \quad (2)$$

where n is the refractive index at 1.5 μm. Fig. 9 shows our estimated $\chi^{(3)}$'s as a function of CsCl concentration. We found a maximum for CsCl content around 30 mol%.

Fig. 2 shows that the glass density increases almost linearly with increasing CsCl concentration. The linear refractive index, which we expect to follow the density, also increases with the CsCl content as shown in Fig. 6. The refractive indices are larger, (3.2–2.2) than the index for silica. The optical non-linearities as predicted by the Lines model [6,7], increase with increasing refractive index. The glass-transition temperatures (T_g) and the softening-point temperature (T_d) are not affected by the CsCl content, but the thermal expansion coefficients (k) reaches a maximum around 30 mol% of CsCl as shown in Fig. 3. Some authors, based on Raman scattering data, assume the formation of $GaS_{1.5}Cl^{1-}$ complex in structure subunits in the glass network [13–15]. The fact that the density, refractive index and thermal expansion coefficient increase with increasing CsCl content, while the optical gap decreases, indicate that CsCl enters the glass structure as a network modifier rather than a glass network former [16].

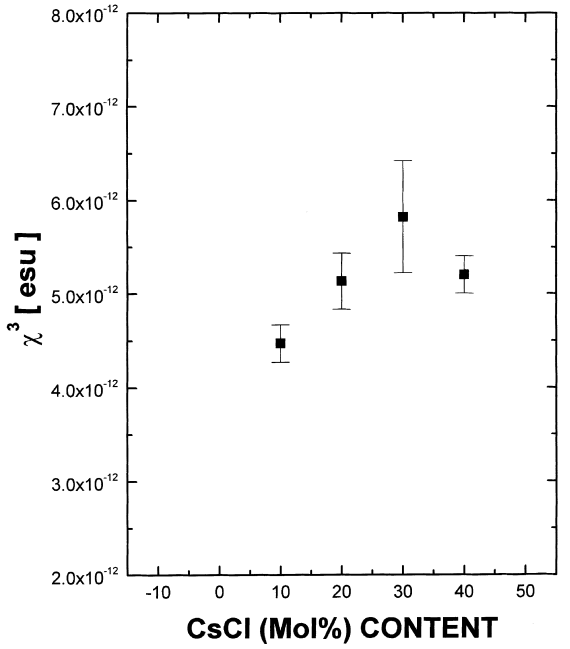

Fig. 9. Third order susceptibility $\chi^{(3)}$ as a function of the CsCl content for GLSC glass system.

Fig. 7 shows the Raman spectra. The band at 315 cm^{-1} is assigned to the breathing mode of $GaS_{1.5}Cl^{1-}$ structure subunits [13,15] (the formation of the $GaS_{1.5}Cl^{1-}$ complex anion maybe due to Ga being fourfold coordinated [14]). We suggest that the band at 85 cm^{-1} is a boson band and the band at 466 cm^{-1} is due to contaminants such as O_2.

We estimate optical non-linearity $\chi^{(3)}$ from Lines' model, Fig. 9. Although these $\chi^{(3)}$s are only estimates, the Lines model has already been successfully compared with experimental data [17].

The most important factor for optical fiber drawing, the thermal stability, given by $T_x - T_g$, increased to ~250°C with increasing CsCl content to a maximum around 30 mol% CsCl, almost 2.5 times larger than the binary system. This difference allowed optical fibers to be drawn from the 30 mol% glass [18].

5. Conclusions

The $20La_2S_3$–$(80 - x)Ga_2S_3$–$xCsCl$ glass system formed glasses with homogeneity and stability in a sulphur atmosphere. The density, refractive index, hardness, glass-transition temperature, thermal expansion coefficient were found to increase with the CsCl content. These trends are consistent with a glass structure in which there are $GaS_{1.5}Cl^{1-}$ structure subunits in which the gallium is fourfold coordinated, with CsCl as a modifier in the network glass. We had to withdraw optical fibers out of this glass system due to an increase of thermal stability with increasing CsCl content.

Acknowledgements

The authors acknowledge Conselho Nacional de Desenvolvimento Científico e Tecnológico (CNPq), Fundação de Amparo à Pesquisa do Estado de São Paulo (FAPESP), Programa de Apoio ao Desenvolvimento Científico e Tecnológico (PADCT), PRONEX and Telecomunicações Brasileiras S/A Telebras, for financial support.

References

[1] P.C. Becker, M.M. Broer, V.G. Lambrecht, A.J. Bruce, G. Nykolak, in: Optical Amplifiers and Their Applications, vol 17, OSA Technical Digest Series, paper no. PDP5 (1992).
[2] B. Dussardier, D.W. Hewak, B.N. Sanson, H.J. Tate, J. Wang, D.N. Payne, Electron. Lett. 31 (3) (1995) 206.
[3] R. Reisfeld, A. Bornstein, Chem. Phys. Lett. 47 (01) (1977) 194.
[4] D.W. Hewak, R.S. Deol, J. Wang, G. Wylangowski, J.A. Medeiros Neto, B.N. Samson, R.I. Laming, W.S. Brocklesby, D.N. Payne, Electron. Lett. 29 (1993) 237.
[5] J. Wang, H.R. Jason, B. Dominic, D. Hewak, B. Brocklesby, M. Kluth, R. Moore, D.N. Payne, Appl. Phys. Lett. 71 (1997) 1753.
[6] M.E. Lines, Phys. Rev. B 43 (1991) 11978.
[7] M.E. Lines, Phys. Rev. B 41 (1990) 3383.
[8] S.H. Wemple, J. Chem. Phys. 67 (1977) 2151.
[9] S.K. Al Ani, C.A. Hogarth, R.A. El Malawany, J. Mater. Sci 20 (1983) 663.
[10] J. Tauc, R. Grigorovici, A. Vancu, Phys. Stat. Sol. 15 (1966) 627.
[11] K. Nassau, Electron. Lett. 17 (1981) 769.
[12] K. Nassau, Bell. Syst. Tech. J. 60 (1981) 327.
[13] Y.S. Tver'yanovich, E.G. Nedoshovenko, V.V. Aleksandov, C.Y. Turkina, A.S. Tver'yanovich, I.A. Sokolov, Glass Phys. Chem. 22 (1) (1996) 9.

[14] A.Y. Tver'yanovich, Y.S. Tver'yanovich, S. Loheidor, J. Non-Cryst. Solids 208 (1996) 49.
[15] E.G. Nedoshovenko, E.Y. Turkina, Y.S. Tver'yanovich, Z.V. Borisova, Vestn Leningrade University, series 4, Fiz Khim. 2 (1986) 52.
[16] V.C.R. Solano, L.C. Barbosa, O.L. Alves, N. Aranha, C.L. Cesar, J. Mater. Chem. 4 (4) (1994) 529.
[17] L. Canioni, L. Sarger, P. Segonds, A. Ducasse, C. Duchesme, E. Fargin, R. Olazeuaga, G. le Flem, Solid State Commun. 84 (1992) 1065.
[18] E.M. Marmolejo, E. Granado, O.L. Alves, C.L. Cesar, L.C. Barbosa, Proceedings of the 18th International Congress on Glass, San Francisco, CA, 1998, pp. 34–38.